ORNL/Sub/94-SS111/02

HIGH TEMPERATURE CORROSION OF ADVANCED CERAMIC MATERIALS FOR HOT GAS FILTERS

Topical Report

for Part 1 of

HIGH TEMPERATURE CORROSION OF ADVANCED CERAMIC
MATERIALS FOR HOT GAS FILTERS AND HEAT EXCHANGERS

December 11, 1997

Report Prepared by
K. E. Spear, C. E. Crossland, D. L. Shelleman and R. E. Tressler
The Pennsylvania State University
Department of Materials Science and Engineering
University Park, PA 16802

under
Subcontract #49X-SS111C

for

DISCLAIMER

Portions of this document may be illegible electronic image products. Images are produced from the best available original document.

HIGH TEMPERATURE CORROSION OF ADVANCED CERAMIC MATERIALS FOR HOT GAS FILTERS

Topical Report

for Part 1 of

HIGH TEMPERATURE CORROSION OF ADVANCED CERAMIC
MATERIALS FOR HOT GAS FILTERS AND HEAT EXCHANGERS

December 11, 1997

Report Prepared by
K. E. Spear, C. E. Crossland, D. L. Shelleman, and R. E. Tressler
The Pennsylvania State University
Department of Materials Science and Engineering
University Park, PA 16802

under
Subcontract #49X-SS111C

for

HIGH TEMPERATURE CORROSION OF ADVANCED CERAMIC MATERIALS FOR HOT GAS FILTERS AND HEAT EXCHANGERS

This program consists of two separate research areas. Part 1, for which this report is written, studied the high temperature corrosion of advanced ceramic hot gas filters, while Part 2 studied the long-term durability of ceramic heat exchangers to coal combustion environments. Since Part 2 of this program is still ongoing, the following paragraphs will only discuss the work performed for Part 1.

Objectives

The objectives of Part 1 were to select two candidate ceramic filter materials for flow-through hot corrosion studies and subsequent corrosion and mechanical properties characterization. In addition, a thermodynamic database was developed so that thermochemical modeling studies could be performed to simulate operating conditions of laboratory reactors and existing coal combustion power plants, and to predict the reactions of new filter materials with coal combustion environments. The latter would make it possible to gain insight into problems that could develop during actual operation of filters in coal combustion power plants so that potential problems could be addressed before they arise.

Service Environments

There are two basic environments that a hot gas filter will encounter. These are oxidizing and reducing. A carbonizing environment is essentially a reducing environment with carbon depositing due to the extreme reducing conditions. This paper will examine six systems currently in use. Three are laboratory operations and three are operating coal combustion plants. Of the six systems, two have been characterized as oxidizing, three as reducing and one as carbonizing. The operating conditions and gas compositions for all six systems are shown in Table 1.

Filter Material

Filters can be classified in two general categories: early and later-generation. Examples of early-generation filters are Schumacher Dia Schumalith FT20 and F40 clay-bonded SiC,

Table1: Operating Conditions and Gas Compositions for Combustion Systems

	Argonne National Lab	Argonne National Lab	Penn State	Pinon Pine	Pinon Pine	Wilsonville Facility
Condition	Oxidizing	Reducing	Oxidizing	Reducing	Reducing	Carbonizing
Temperature	850°C	650°C	870°C	750°C	750°C	816°C
Pressure	1 atm	1 atm	1 atm	1 atm	10 atm	11.6 atm
N_2	72.4 %	50 %	-	48.66 %	48.66 %	52.60 %
CO_2	13.5 %	6.9 %	-	5.45 %	5.45 %	23.7 %
CO	-	8.8 %	-	23.89 %	23.89 %	6.8 %
O_2	3.7 %	-	30 %	-	-	-
H_2O	10.5 %	24 %	15 %	5.51 %	5.51 %	12.5 %
H_2	-	9.4 %	-	14.57 %	14.57 %	0.5 %
SO_2	250 ppm	-	3300 ppm	-	-	-
H_2S	-	-	-	20 ppm	20 ppm	0.08 %
NaCl	50 ppm	50 ppm	10 ppm	-	-	30 ppm
CH_4	-	-	-	1.35 %	1.35 %	1.6 %
NH_3	-	-	-	0.02 %	0.02 %	0.08 %
Other	-	-	HCl - 1100 ppm Air - Balance	Ar - 0.56 %	Ar - 0.56 %	COS - 0.015 % C_{2+} - 2.1 %

Coors P-100A alumina/mullite and Pall Vitropore 442T clay-bonded SiC. The DuPont/Lanxide PRD-66 filament-wound oxide (layered cordierite, mullite, cristobalite and corundum), DuPont/Lanxide 'enhanced SiC-SiC' and 3M Type 203 CVI-SiC composite are considered later-generation filters. A summation of different filter types and where they have been tested has been presented previously by Alvin [1]. An updated list is shown in Table 2. The two candidate filters studied in this program were DuPont/Lanxide 'enhanced SiC-SiC' and 3M Type 203 CVI-SiC composite.

Experimental Procedure

Based on results from earlier flow-over tests on 3M's Type 203 filters (SiC matrix-Nextel fiber composite) and DuPont Lanxide's SiC-SiC composite filters with Nicalon fibers, a reactor was developed to allow for flow-through experiments on 18" sealed sections of filters coated with ash collected at the Tidd plant. The vertical flow-through reactor schematically shown in Figure 1 consists of a 6 inch I.D. SiC furnace

Table 2: Common First and Second-Generation Filters and Test Locations

| Process	Operating Condition	Temp. Range (°C)	Candle Filter Type	Test Facility
AEP Tidd PFBC	Oxidizing	620-845	FT20, F40, 442T, P-100A, PRD-66, Type 203	Demonstration Plant
Karhula PCFBC	Oxidizing Oxidizing	850-900 690-850	P-100A 442T	Pilot Plant
FW PFBC	Oxidizing	700-870	F40, P-100A	Pilot Plant
FW Carbonizer	Carbonizing	<760	P-100A	Pilot Plant
Texaco Gasifier	Reducing	700	F40, P-100A	Pilot Plant
Pinon Pine	Reducing	750		Pilot Plant
Wilsonville	Carbonizing	816		Pilot Plant
Argonne National Lab	Oxidizing Reducing	850 650		Laboratory
Penn State	Oxidizing	870	Type 203, D/L 'enhanced SiC-SiC'	Laboratory
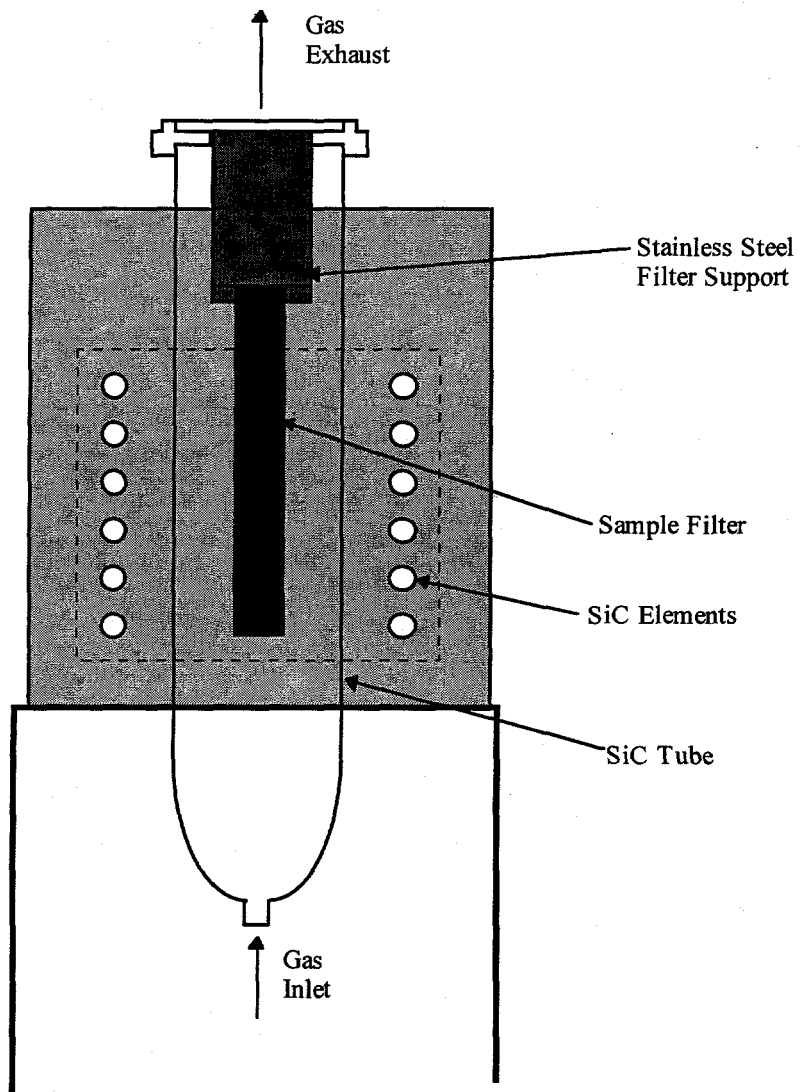
Figure 1. Vertical flow-through reactor designed for corrosion studies of cermaic filters.

tube fixed at the exhaust end by a stainless steel cylinder to support the filter sections. The 1 atmosphere inlet gas flow of 30% O_2, 15% H_2O, 3300 ppm SO_2, 1100 ppm HCl, 10 ppm NaCl and 55% air is forced to flow through the filter material. According to Hurley [2], these are the primary species which must be included in PFBC hot-gas filter tests since they either corrode silicon- and aluminum-based ceramics, or affect the activities of the corrodents. The above concentrations are those suggested by Hurley for 1 atm tests.

The presently described Penn State tests were carried out with the inlet gas flow rate between 1 and 5 slm at temperatures up to 870°C and time periods of 50, 100 and 200 hours. After exposure to the corrosive environment, any phase or morphological changes were studied with x-ray diffraction and scanning electron microscopy. The residual strength of the filters were measured by internal pressurized burst testing.

Results and Discussion

Flow-Through Test

An initial flow-through test has been conducted on a section of 3M Type 203 filter at 870°C and 5 slm for 50 hours. Figure 2 contains a scanning electron micrograph of the inner surface of the filtering layer of the as-received 3M filter. The filtering layer consists of a mat of chopped Nextel 312 fibers with a CVI layer of SiC. The fiber surfaces appear smooth with spherical features on the order of 5 microns. Figure 3 shows the inner surface of the filtering layer after exposure. The mat now consists of 1 micron diameter fibrils extending from the chopped fiber surface.

Constant volume x-ray powder diffraction of the filtering layer of the as-received 3M filter revealed the presence of alpha SiC. The SiC is likely a mix of polytypes but the x-ray pattern most closely matches that of the 15R polytype (JCPDS file number 39-1196). X-ray on the exposed 3M filtering layer revealed an amorphous or glassy component and several low-angle peaks in addition to the SiC peaks found in the as-received 3M filter (Figure 4). The low-angle peaks seem to indicate the presence of trace amounts of tridymite.

Strength Testing

As-received and exposed 3M filter materials were cut into 4" sections for internal pressurized burst testing. To pressurize the tubes from these materials, 3 inch rubber plugs were made and centered 0.5 inches from each end to minimize edge effects. The ends of the plugs were then compressed at a crosshead speed of 5 mm/min until the tube sections failed. Results indicate that the exposed filter maintained approximately 85 % of its initial strength.
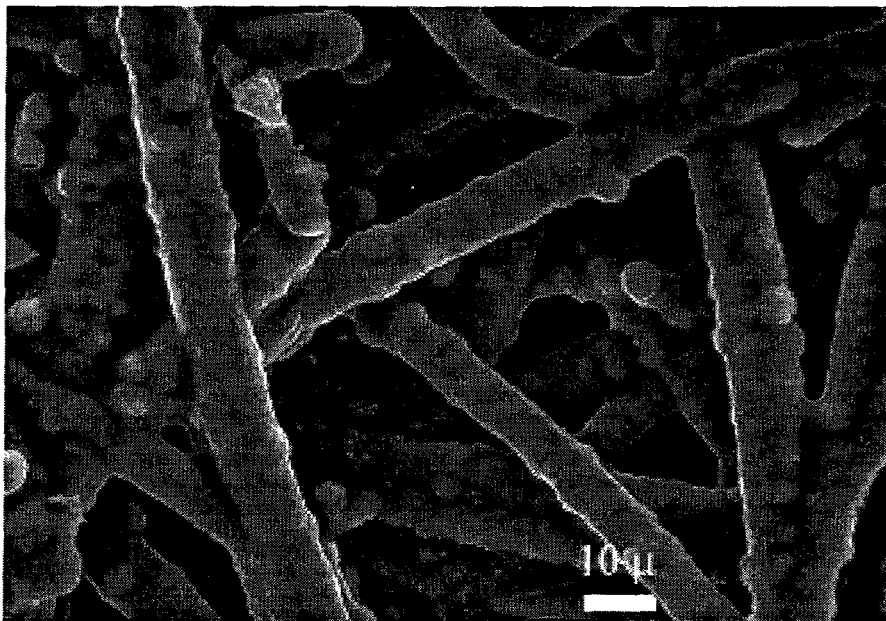
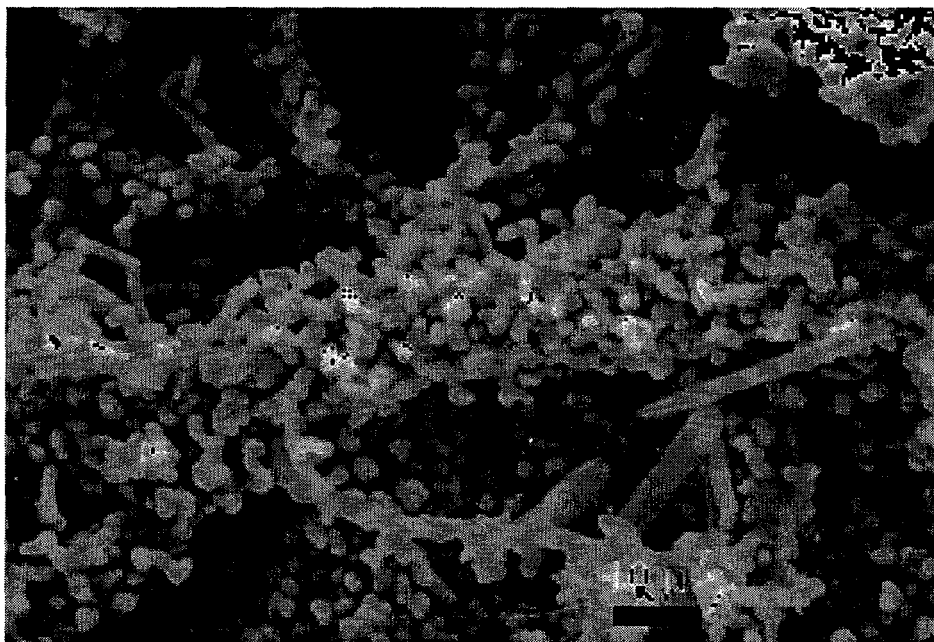Figure 2. Filtering layer of as- received 3M Type 203 filter.

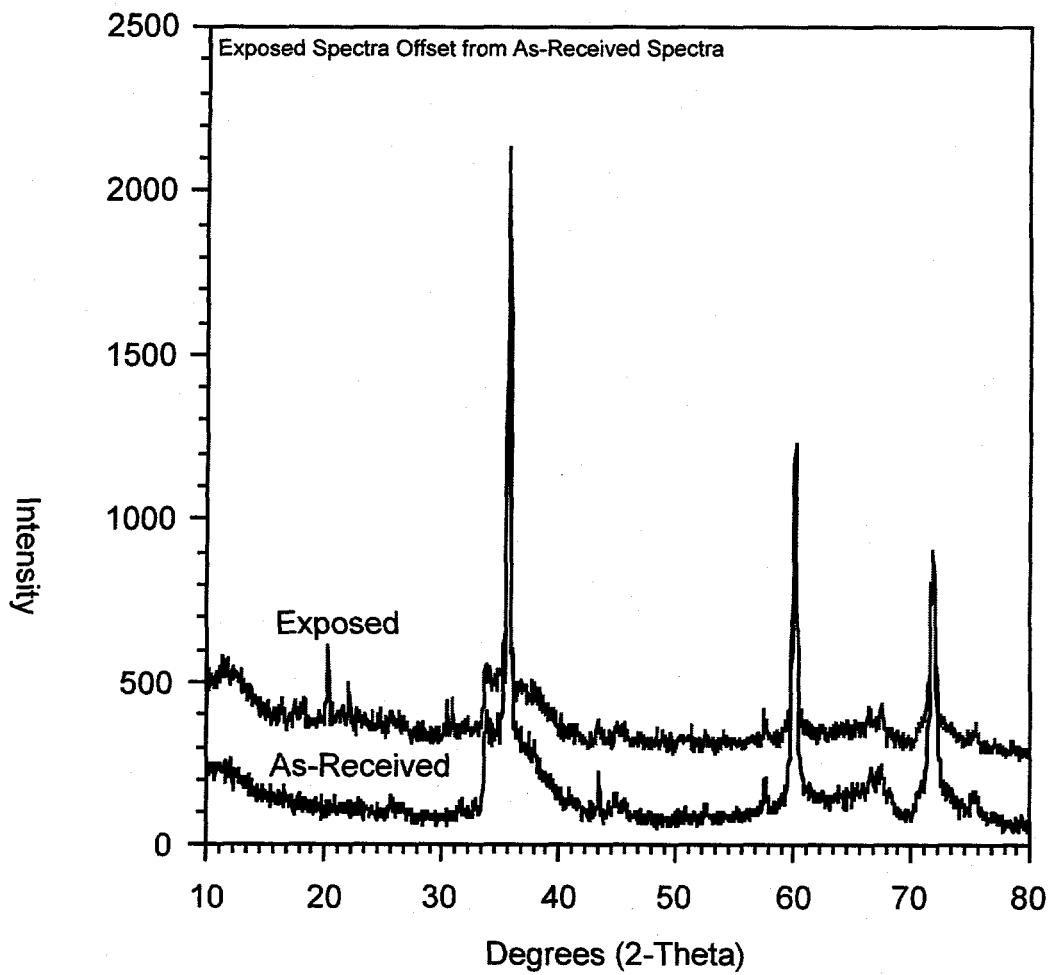Figure3. Filtering layer of 3M Type 203 filter after exposure at 870°C for 50 hours.

Figure 4. Powder X-ray diffraction patterns of as-received and exposed filtering layer from 3M Type 203 filters.

Thermochemical Modeling

Oxidation/corrosion of ceramic materials is a major concern when designing hot-gas filters. The effect of temperature, pressure, steam, sulfur and alkali concentration is of great importance. By using thermochemical modeling, the limiting reactions of the ceramic materials in oxidizing and reducing systems can be predicted in advance of actual field trials. The reactions of silicon carbide filters and alumina/mullite filters with several oxidizing and reducing atmospheres (Table 1) were examined using ChemSage equilibrium software and thermodynamic data from the SGTE database [3], with the exception that the data for the Si-O-H molecules were taken from Allendorf et al. [4]. These hydroxide data are consistent with experimental results of Opila et al. [5] and Krikorian [6]. Appendix A contains a complete input/output of a typical calculation to illustrate the extensive number of gaseous and condensed species which were considered. The Penn State gas composition/conditions listed in Table 1, along with excess solid SiC were used for this calculation.

Two types of information were examined in the modeling calculations. First, we determined if any solid products were formed at equilibrium in addition to the solids which were added in excess to the input species. Second, for the SiC filter corrosion simulations, we identified the most important gaseous species (and their partial pressures) which contained Si, S, Na, and Cl. For the alumina/mullite simulations, the most important gas containing Al was added to the above list. These respective data are summarized in Tables 3 and 4, and will be discussed below. More detailed information concerning other important species is given in respective Appendices B and C. Although many gaseous species are present at equilibrium with each filter material, as is clearly illustrated by the listing in Appendix A, only the important gases containing sodium, chlorine, sulfur, silicon and aluminum are shown in Appendices B and C. These are the gases directly related to the degradation of the filter materials.

Figure 5 schematically shows the reaction interfaces encountered by the combustion gases over time as interactions with SiC-based filters occur, and is the basis for the logic of our thermochemical modeling calculations. The initial interaction of the gases with the filter oxidizes the SiC to form SiO_2 and carbon. This occurs even with "reducing" gas mixtures. Over time, the carbon will typically be oxidized and a protective coating of the SiO_2 will cover the SiC filter. Thus, at later stages, the input of fresh combustion gases to the filter will primarily interact with the protective oxide coating.

Our SiC filter modeling studies considered the two extreme cases for each condition shown in Table 1: (a) equilibration of the combustion gases with excess SiC, and (b) equilibration of the same input combustion gases with excess SiO_2. Table 3 provides a summary of these SiC filter modeling results. Condensed versions of the input and output results for these calculations are given in Appendix B.

Table 3: Summary of Thermodynamic Modeling Results for Simulating the Corrosion of SiC Hot-Gas Filter Materials

| Facility | Operating Conditions* | | | | | EQUILIBRIUM PHASES AND SPECIES Gas/P(atm) of most abundant species containing: | | | |
	Condition	T°C	P(atm)	Filter	additional solids	Si	S	Na	Cl
Argonne	Oxidizing	850	1.0	none	Na_2SO_4	not present	SO_2/2.1E-4	NaCl/1.5E-6	HCl/4.8E-5
Argonne	Reducing	650	1.0	none	NaCl	not present	not present	NaCl/7.0E-6	NaCl/7.0E-6
Argonne	Oxidizing	850	1.0	SiC	C/SiO_2	SiS/1.7E-5	H_2S/2.8E-4	NaCl/5.6E-5	NaCl/5.6E-5
				SiO_2 film	Na_2SO_4	$Si(OH)_4$/9.3E-9	SO_2/2.1E-4	NaCl/1.5E-6	HCl/4.8E-5
Argonne	Reducing	650	1.0	SiC	C/SiO_2/NaCl	SiH_3Cl/1.1E-10	not present	NaCl/7.0E-6	NaCl/7.0E-6
				SiO_2 film	$Na_2Si_2O_5$	$Si(OH)_4$/8.7E-9	not present	NaCl/2.5E-6	HCl/4.7E-5
Penn State	Oxidizing	870	1.0	SiC	C/SiO_2	SiS/2.4E-4	H_2S/5.3E-3	NaCl/1.7E-5	HCl/1.9E-3
				SiO_2 film	Na_2SO_4	$Si(OH)_4$/2.1E-8	SO_2/2.6E-3	NaCl/7.5E-6	HCl/1.1E-3
Pinon Pine	Reducing	750	1.0	SiC	C/SiO_2	SiS/8.5E-8	H_2S/2.8E-5	not present	not present
				SiO_2 film	----	$Si(OH)_4$/5.9E-10	H_2S/1.9E-5	not present	not present
Pinon Pine	Reducing	750	10.0	SiC	C/SiO_2	SiS/1.1E-7	H_2S/2.9E-4	not present	not present
				SiO_2 film	C	$Si(OH)_4$/2.0E-7	H_2S/2.0E-4	not present	not present
Wilsonville	Carbonizing	816	11.6	SiC	C/SiO_2	SiS/2.7E-5	H_2S/1.6E-2	NaCl/3.2E-4	NaCl/3.2E-4
				SiO_2 film	$Na_2Si_2O_5$	$Si(OH)_4$/1.2E-6	H_2S/1.0E-2	NaCl/4.2E-5	HCl/3.0E-4

* See Tabe 1 for more details on operating conditions.

Table 4: Summary of Thermodynamic Modeling Results for Simulating the Corrosion of Alumina/Mullite Hot-Gas Filter Materials

	Operating Conditions				additional	--------EQUILIBRIUM PHASES AND SPECIES-------- Gas/P(atm) of most abundant species containing:			
Facility	Condition	T°C	P(atm)	Filter	solids	Si/Al	S	Na	Cl
Argonne	Oxidizing	850	1.0	Al_2O_3/mull	$NaAlSiO_4$	$Si(OH)_4$/5.3E-9 $Al(OH)_3$/2.9E-11	SO_2/2.3E-4	NaCl/8.2E-7	HCl/4.9E-5
Argonne	Reducing	650	1.0	Al_2O_3/mull	$NaAlSiO_4$	$Si(OH)_4$/4.1E-9 $Al(OH)_3$/8.9E-13	not present	NaCl/3.8E-8	HCl/5.0E-5
Penn State	Oxidizing	870	1.0	Al_2O_3/mull	Na_2SO_4	$Si(OH)_4$/1.2E-8 $Al(OH)_3$/7.0E-11	SO_2/2.6E-3	NaCl/7.5E-6	HCl/1.1E-3
Pinon Pine	Reducing	750	1.0	Al_2O_3/mull	----	$Si(OH)_4$/3.0E-10 $Al(OH)_3$/7.7E-13	H_2S/1.9E-5	not present	not present
Pinon Pine	Reducing	750	10.0	Al_2O_3/mull	C	$Si(OH)_4$/1.0E-7 $Al(OH)_3$/6.1E-11	H_2S/2.0E-4	not present	not present
Wilsonville	Carbonizing	816	11.6	Al_2O_3/mull	$NaAlSiO_4$	$Si(OH)_4$/6.8E-7 $Al(OH)_3$/6.9E-10	H_2S/1.0E-2	NaCl/1.1E-6	HCl/3.4E-4

* See Tabe 1 for more details on operating conditions.

11

Combustion Gas

SiC

SiC

SiO$_2$

SiO$_2$

SiO$_2$
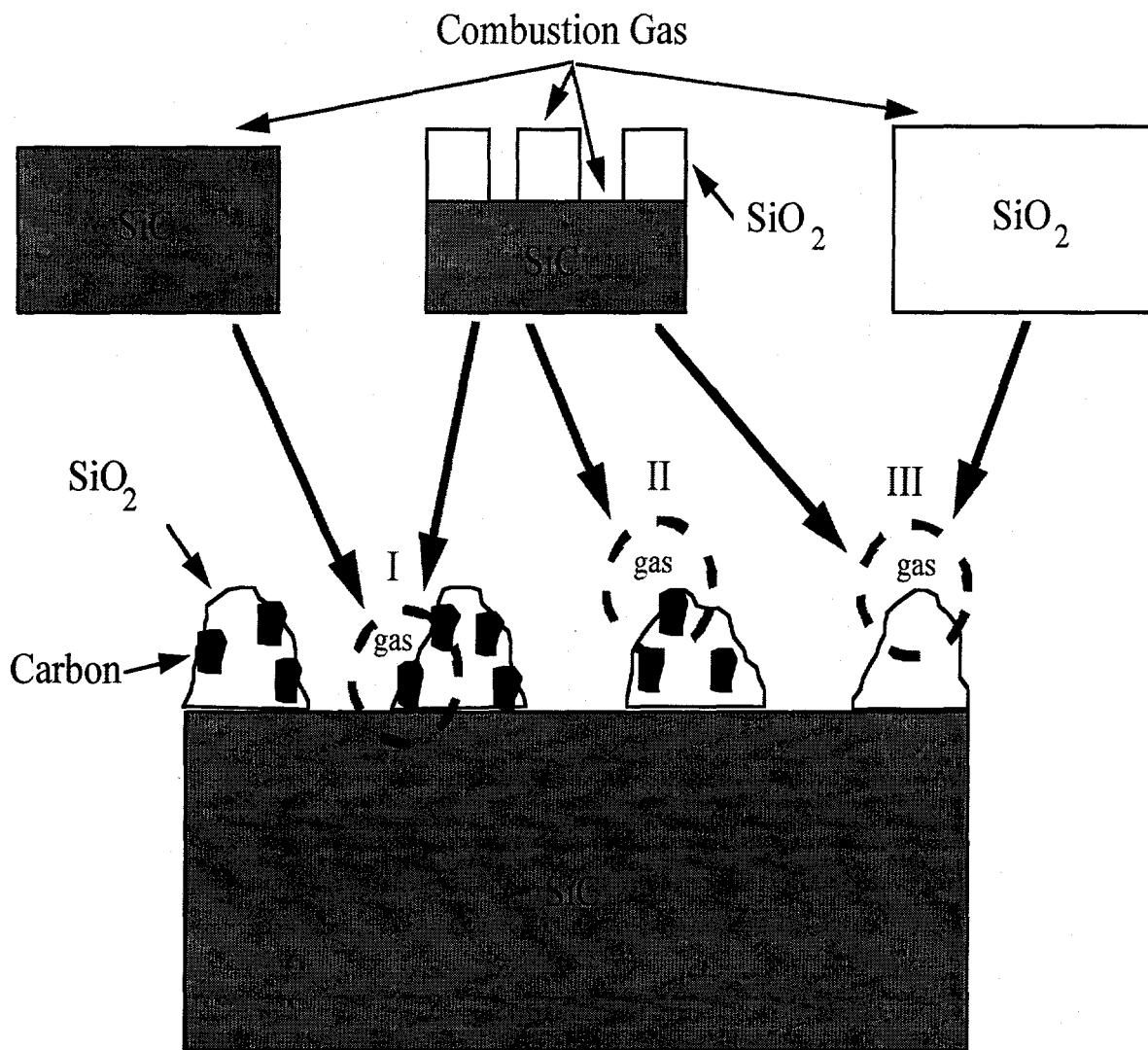
Carbon

I
gas

II
gas

III
gas

SiC

Figure 5. Schematic of reaction interface for combustion gases with SiC-based filters.

Our alumina/mullite filter modeling studies considered each condition shown in Table 1 along with excess alumina/mullite. Table 4 provides a summary of these alumina/mullite filter modeling results. Condensed versions of the input and output results for these calculations are given in Appendix C.

Table 3 summarizing our SiC filter modeling results shows that the initial reactions of a combustion gas with the filter always produce a reducing environment at the equilibrium gas/filter interface. The equilibrium mixture consists of the gas, excess SiC, and product solid phases of SiO_2 and C. Other solid product phases may also form, as is seen in Table 3. Under these reducing conditions, the sulfur from the combustion gas is primary in the form of gaseous H_2S, and the most important Si-containing gas under these condition is SiS. Sulfur is present in every system considered, except the Argonne reducing environment. The calculated partial pressure of SiS(g) is actually several orders of magnitude greater than that of silicon oxide, SiO(g) (see Appendix B for results of calculations with excess SiC). Therefore, sulfur can have a great influence on the removal of silicon from SiC. These results are typical for all conditions considered which produced a reducing environment.
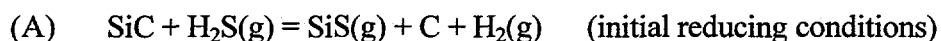
If the SiC from the filter does not equilibrate with the combustion gas, as is the case after a protective SiO_2 oxide coating forms on the filter, then our model assumes the combustion gas equilibrates with excess silica glass in the filter region. Under the oxidizing Penn State conditions, solid Na_2SO_4 is also predicted to form and the primary sulfur containing gas is SO_2. This result was also obtained for the oxidizing gas used at Argonne. All other conditions listed in Table 3 which were modeled produced a reducing gas environment, even when the protective SiO_2 film formed on the filter. No solid Na_2SO_4 was predicted at equilibrium under these reducing conditions. This was true, for example, for the Pinon Pine and Wilsonville conditions both before and after a protective SiO_2 coating forms on the filter.

For equilibrium conditions after a protective SiO_2 coating forms on the filter, solid $Na_2Si_2O_5$ was predicted in two cases, and free carbon in another. Under 1 atm conditions, the Pinon Pine gas did not produce solid carbon when the protective oxide film was present, but did precipitate carbon under the same conditions at 10 atm total pressure. The "carbonizing" gas of the Wilsonville plant did not produce solid carbon with its 11.6 atm total gas pressure when the protective silica film was present. The NaCl concentration used in the reducing gas conditions at Argonne was high enough to produce NaCl solid along with the SiC oxidation products of SiO_2 and C.

Although sodium does not play an active role in silicon removal from the system, in several cases, a condensed sodium sulfate, sodium chloride, or sodium silicate was predicted to form, particularly after the protective silica oxidation layer was in place. Sodium may act as a fluxing agent on the surface of a filter thus affecting the diffusion of

oxygen or water vapor through the silica layer and may promote the retention of ash on the filter surface [8].

The maximum loss of SiC filter material by gaseous corrosion products can be predicted using the equilibrium partial pressures of the most abundant silicon containing species. When the gas initially equilibrates with the excess SiC, producing reducing conditions at the gas/filter interface, Table 3 shows that SiS gas is the most abundant silicon-containing species when sulfur is present. When the protective silica film forms on the filter, gaseous $Si(OH)_4$ is the most abundant silicon-containing species. Under the 1 atm conditions used in most of the modeled systems, the initial filter loss rates from SiS formation are predicted to be orders of magnitude greater than the later loss rates from gaseous $Si(OH)_4$, which dominates after a protective oxide coating forms. However, increases in the total system pressure cause these two rates to be more comparable, as is seen by comparing the Pinon Pine 1 atm and 10 atm results. The SiS pressure does not change much with an increase in pressure, while the $Si(OH)_4$ pressure increases by several orders of magnitude. The two chemical reactions of relevance are:

(A) $SiC + H_2S(g) = SiS(g) + C + H_2(g)$ (initial reducing conditions)

(B) $SiO_2 + 2 H_2O(g) = Si(OH)_4(g)$ (after protective SiO_2 film forms)

In reaction (A), an increase in the H_2:H_2S ratio with increasing total pressure is needed to cause an increase in the SiS pressure with increasing total pressure. If the respective fractions of the H_2 and H_2S in the gas stay constant as total pressure increases, their individual partial pressures would increase, but not their ratio, so the SiS partial pressure would remain constant.

With reaction (B), an increase in the partial pressure of H_2O will cause an increase in the $Si(OH)_4$ partial pressure. Again, if the fraction of the H_2O in the gas stays constant as total pressure increases by say an order of magnitude, the H_2O partial pressure would also increase by an order of magnitude, and the partial pressure of $Si(OH)_4$ would increase by two orders of magnitude.

Of course, assuming the above gas species fractions stay constant with increasing total pressure is a simplification since other reactions involving these species are also a function of pressure. However, the main point to be made is that the $Si(OH)_4$ partial pressure has a much stronger dependence on total pressure than the SiS partial pressure.

The modeling calculations and the above discussion point out the important role that sulfur can have on silicon removal when strong reducing conditions exist (excess SiC). However, the "reducing" combustion gases listed in Table 1 are not reducing enough for $SiS(g)$ to dominate the silicon removal when a protective silica coating forms on the filter. Therefore, this SiS corrosion mechanism is controlled by the rate at which the protective

silica layer forms. Under these latter conditions, $Si(OH)_4$ gas dominates the silicon removal via the vapor phase. As noted above with reaction (B), water vapor has a strong influence on the $Si(OH)_4$ partial pressure.

This above influence of water vapor on SiO_2 corrosion was experimentally observed previously for reactions with a 10% H_2O/10% O_2/ 80% N_2 atmosphere at temperatures up to 1100°C at 1 atm total pressure and up to 1300°C at 10 atm total pressure [6-7]. The removal of silicon from the filter by SiS(g) under excess SiC conditions is several orders of magnitude larger than would occur by the active oxidation of SiC by SiO(g) (see data in Appendix B for excess SiC conditions). This indicates the severe corrosive effect that sulfur can have on SiC. It should be noted that the $Si(OH)_4$ gas partial pressures which dominate the silicon removal when a protective silica layer is formed are at least as great or greater than the partial pressures of SiO gas which exist during the active oxidation of SiC (see data in Appendix B for excess SiC conditions).

An alumina/mullite filter material examined under the same above conditions that were considered for SiC-based filters revealed the loss of aluminum and silicon through the gases $Al(OH)_3$ and $Si(OH)_4$, as is shown in Table 4. The $Si(OH)_4$ partial pressures produced by reaction with mullite were the same order of magnitude as the cases in which a protective silica coating was present in the SiC system. These partial pressure values are expected for alumina/mullite filters since the thermodynamic activity of silica is calculated to be ~0.5 for all conditions examined with these materials (see Appendix C).

The $Si(OH)_4$ (g) partial pressures were always several orders of magnitude greater than those of $Al(OH)_3$, which indicates the surface of the mullite could become rich in Al_2O_3 with time, providing a more corrosion-resistant surface layer. A factor of 10 pressure increase for the Pinon Pine reactor (Table 4, Appendix C), increased the $Si(OH)_4$ (g) by about 300, and the $Al(OH)_3$ (g) by about 100. This effect of total pressure is explained by the H_2O pressure increase of about 20, and the reactions of the water with the oxides to form their respective hydroxides.

Solid $NaAlSiO_4$ was predicted to form in several cases of modeling the corrosion of alumina/mullite filters, and Na_2SO_4 was predicted to form in one case. Alvin et al. [8] predicted that oxide-based materials would react with gas-phase alkali forming stable solid complexes. As was mentioned above, sodium may flux the surface of the filter and promote reactions and retention of ash on the filter surface. Sulfur did not have any noticeable effect on the corrosion reactions of the alumina/mullite filter material.

Comparison with Other Studies and Field Experience

The above thermochemical calculations of possible corrosion reactions should ideally be compared in detail to data from other modeling studies, experiments and field experience. The most extensive thermochemical modeling on these systems reported previously was

that of Judkins et al. [7]. They recently reviewed the use of silicon carbide hot-gas filters in coal gasification and pressurized fluidized bed combustion environments, and also performed thermodynamic calculations to examine the stability of various ceramic phases. Quantitative comparisons of their PFBC results with those reported here are not possible since: (a) a complete listing of the chemical species used in their dataset was not given, (b) they used 1 MPa pressure while we used 1 atm (~0.1 MPa), and (c) their input gas composition was different from ours. Both studies used a temperature of 870°C. Also, the logic of Judkins et al. [7] simulations was not specified, so it is not clear how the input concentrations were determined in order to simulate the gas-solid interface reactions expected to occur in a dynamically reacting flow system. Some of these points are briefly discussed below to illustrate the problems with attempting to quantitatively compare the two studies.

For example, Table 3 summarizing our modeling results for SiC filters shows that the initial reactions of the combustion gas with the filter produces a reducing environment in which the equilibrium typically consists of the gas, excess SiC, and product solid phases of SiO_2 and C. The sulfur is primary in the form of gaseous H_2S, and the most important Si-containing gas under these reducing conditions is SiS. The species H_2S and SiS are not mentioned as being important in the review of Judkins et al. [7], but it is not known why their results were different; perhaps these species were not included in their thermodynamic dataset, or they did not perform calculations with excess solid SiC. The formation of gaseous H_2S and SiS under the reducing conditions which occur at the SiC-gas interface reduces the tendency for solid Na_2SO_4 to form.

The influence of increasing the system pressure was discussed above, and is most dramatic in the increase in the $Si(OH)_4$ partial pressure since it will increase by the square of the increase in water partial pressure. This hydroxide species was not included in the discussions of Judkins et al. [7], but it is probably the most important cause of silicon loss from SiC filters once a protective oxide layer is formed.

In our laboratory studies, accelerated oxidation of SiC has been observed due to the presence of H_2O and alkalis. This results in the accelerated formation of SiO_2, silicates, and sulfates. At temperatures of 870°C and 200 hours of exposure, tridymite began to crystallize in conjunction with the formation of an amorphous, glassy phase on the surface of the SiC filters. EDAX analysis of the glassy material indicated the presence of silicon, oxygen, sulfur, magnesium, potassium and aluminum. The magnesium, potassium, and aluminum are from the ash and formed a solid solution with the SiO_2 glassy phase (Figures 2 & 3). Since we did not consider ash in our modeling studies, a direct comparison of our experiments and modeling results cannot be made. However, these two sets of results are consistent with one another, and in good qualitative agreement.

16

Alvin has reported oxidation of SiC based filter at temperatures of 620-870°C [1,8]. The presence of gas phase sodium appeared to enhance surface oxidation of the SiC leading to areas enriched with SiO_2. However, sodium was not detected in the SiO_2 layer after 400 hours of exposure to a 20 ppm NaCl/steam/air flow-through environment at 870°C [1] nor in 200 hour flow-through tests at Penn State under similar conditions (Table 1). The vapor pressure of NaCl was apparently high enough to vaporize sodium away from the glass by a reaction such as that given below, thus preventing the formation of the sodium silicate.

$$(C) \quad Na_2Si_2O_5 + 2\,HCl(g) = 2\,NaCl(g) + H_2O(g) + 2\,SiO_2$$
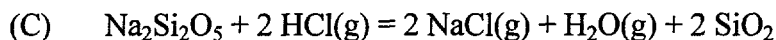
Also exchange reactions of potassium from the ash with the sodium may play a role in the sodium loss to the vapor. The predictions of volatilization of oxides via hydrated species, particularly at high system pressures, requires monitoring of weight loss during service or high-pressure experiments. These types of experiments have not been performed but based on SEM observations before and after exposure [8], bondposts between grains in clay-bonded SiC materials appear to have thinned, indicating a loss of silica.

The extent to which the observed degradation of mechanical properties is due to these possible corrosive reactions is not clear at this point since the carefully controlled experiments at high system pressures have not been performed. There is a need to test these predictions by careful experiments and observations of field tests of materials before and after field exposure.

Conclusions

Thermochemical modeling of the reaction of corrosive environments with ceramic hot gas filer materials used in coal combustion power generating systems can be effectively used to predict the effects of temperature, pressure, and gas constituents on the chemical stability of the filter material. These predictions can then be used to anticipate problems that may arise during actual operating conditions not easily duplicated in a laboratory setting such as the extreme pressures found in an operating coal combustion plant. Our modeling has shown that sulfur can play a very active role in the removal of silicon from SiC by forming SiS(g) during the initial stages of corrosion, and that water vapor can produce significant partial pressures of $Si(OH)_4$ from reactions with (a) silica protective coatings on SiC filters, and (b) silica in the mullite. Sodium does not directly affect the removal of silicon, but may act as a fluxing agent by forming sodium sulfates, chlorides, or silicates on the surface of the filters which could than alter the diffusion of oxygen and water vapor through the glassy interface, as well as promote the sticking of ash particles. The removal of aluminum from alumina/mullite by hydroxide gaseous species is almost three orders of magnitude less severe than the removal of silicon by its hydroxides. In order to develop a complete understanding of the corrosion of ceramic filters, further

17

work is needed in modeling the slag solid solutions that the ash forms on the filter surface during particulate removal.

The above thermodynamic predictions provide the limiting equilibrium behavior of these filter materials in a corrosive environment. Kinetic factors were qualitatively discussed in terms such "protective coatings" which slow reaction rates, but more thought and modeling is needed in this area. Also, maximum corrosion rates through vapor losses could be calculated by assuming the vapor is saturated with the equilibrium gaseous species. This is probably a good assumption since the gas has significant contact time with the filter while it is passing through the filter. These predictions should be used as guidelines in designing experimental programs and pilot plant tests.

References

1. Alvin, M. A., "Porous Ceramic Hot Gas Filters - Materials and Applications," *Proc. 2nd Int. Conf. on Heat-Resistant Materials*, Gatlinburg, TN, 525-536, (1995).

2. Hurley, J.P., "Annual Technical Progress Report," *Support Services for Ceramic Fiber-Ceramic Matrix Composites,* **ORNL/Sub/94-SS112/01**, September 20, 1995, pp. 10-11.

3. Eriksson, G., (a) ChemSage© Application Software for Thermochemical Calculations, Version 3.0.1, (b) SGTE Pure Substance Database; GTT TECHNOLOGIES, Kaiserstrasse 100, D-52134 Herzogenrath, Germany, 1994.

4. Allendorf, M.D., Melius, C.F., Ho, P., and Zachariah, M., "Theoretical Study of the Thermochemistry of Molecules in the Si-O-H System," *J. Phys. Chem.* **99**, 15285 (1995).

5. Opila, E. J. and Jacobson, N. S., "Volatile Hydroxide Species of Common Protective Oxides and Their Role in High Temperature Corrosion," In ECS Proceedings Volume 96-26, *Fundamental Aspects of Corrosion VI* (D.A. Shores, R.A. Rapp, and P. Hou, eds.), The Electrochemical Society, Pennington, NJ (1996).

6. Krikorian, O.H., "Thermodynamics of Silica-Steam System," *Symposium on Engineering with Nuclear Explosives,* January 14-16, 1970, Las Vegas, NV (Unpublished), Vol. 1, pp. 481-492.

7. Judkins, R.R., Stinton, D.P., and DeVan, J.H., "A Review of the Efficiacy of Silicon Carbide Hot-Gas Filters in Coal Gasification and Pressurized Fluidized Bed Combustion Environments," *Trans. ASME* **118**, 500-506 (1996).

8. Alvin M. A. , Lippert, T. E. and Lane, J. E., "Assessment of Porous Ceramic Materials for Hot Gas Filtration Applications," Ceram. Bull., **70** [9] 1491-1498 (1991).

APPENDIX A

Table A1.   Detailed input/output of equilibrium calculation for Penn State
gases present with excess SiC filter material. Details of conditions
are given in Table 1. Summary results are given in Table 3. This
example illustrates the extensive number of gaseous and condensed
species which are considered in each equilibrium calculation.

Table A1: Complete set of results obtained when calculating the equilibrium for the Penn State conditions (Table 1) with excess SiC.

Penn State   SiC Filter   kes/psu 11/24/97

T = 870.00 C
P = 1.00000E+00 atm
V = 5.53780E+03 dm3

STREAM CONSTITUENTS	AMOUNT/mol
N2/Gas/	4.4000E+01
O2/Gas/	4.1000E+01
H2O/Gas/	1.5000E+01
O2S/Gas/	3.3000E-01
ClNa/Gas/	1.0000E-03
ClH/Gas/	1.1000E-01
CSi	1.0000E+02

EQUIL AMOUNT MOLE FRAC PRESSURE

PHASE: Gas

Species	EQUIL AMOUNT mol	MOLE FRAC	PRESSURE atm	Species	EQUIL AMOUNT mol	MOLE FRAC	PRESSURE atm
N2	4.4000E+01	7.4531E-01	7.4531E-01	OSi	1.6350E-07	2.7695E-09	2.7695E-09
H2	1.4504E+01	2.4567E-01	2.4567E-01	CCl2H4Si	1.4931E-07	2.5291E-09	2.5291E-09
H2S	3.1556E-01	5.3452E-03	5.3452E-03	Na	5.8175E-08	9.8542E-10	9.8542E-10
ClH	1.0994E-01	1.8623E-03	1.8623E-03	CClH3	5.5971E-08	9.4809E-10	9.4809E-10
CH4	9.0423E-02	1.5317E-03	1.5317E-03	Cl	1.2619E-08	2.1375E-10	2.1375E-10
SSi	1.4363E-02	2.4329E-04	2.4329E-04	S	6.2019E-09	1.0505E-10	1.0505E-10
ClNa	9.8937E-04	1.6759E-05	1.6759E-05	H4Si	2.4584E-09	4.1642E-11	4.1642E-11
CO	7.1047E-04	1.2035E-05	1.2035E-05	Cl3Si	1.1675E-09	1.9775E-11	1.9775E-11
HS	3.9487E-05	6.6887E-07	6.6887E-07	C2ClH7Si	4.6555E-10	7.8859E-12	7.8859E-12
ClH3Si	3.6061E-05	6.1084E-07	6.1084E-07	CO2	3.7998E-10	6.4365E-12	6.4365E-12
S2	2.0942E-05	3.5474E-07	3.5474E-07	CH2O	9.1602E-11	1.5516E-12	1.5516E-12
H2O	9.0531E-06	1.5335E-07	1.5335E-07	C3H8	3.1616E-12	5.3555E-14	5.3555E-14
Cl2Na2	5.2871E-06	8.9558E-08	8.9558E-08	C2ClH5	1.9859E-12	3.3639E-14	3.3639E-14
Cl3HSi	3.6877E-06	6.2466E-08	6.2466E-08	C2Cl2H6Si	1.0704E-12	1.8132E-14	1.8132E-14
Cl2Si	1.2219E-06	2.0697E-08	2.0697E-08	Cl2	4.2442E-13	7.1892E-15	7.1892E-15
Cl4Si	9.4625E-07	1.6028E-08	1.6028E-08	CH4O	2.6861E-13	4.5499E-15	4.5499E-15
COS	6.8155E-07	1.1545E-08	1.1545E-08	O2Si2	6.3724E-14	1.0794E-15	1.0794E-15
Cl2H2Si	3.8117E-07	6.4565E-09	6.4565E-09	HNaO	2.3360E-14	3.9569E-16	3.9569E-16
C2H6	3.0205E-07	5.1164E-09	5.1164E-09	CCl2H2	1.9293E-14	3.2680E-16	3.2680E-16
CCl3H3Si	2.4880E-07	4.2145E-09	4.2145E-09	H4O2Si	1.5975E-14	2.7059E-16	2.7059E-16

Species			
Si	1.0176E-14	1.7237E-16	1.7237E-16
OS2	6.1095E-15	1.0349E-16	1.0349E-16
CClHO	4.5152E-15	7.6483E-17	7.6483E-17
Cl2S	1.9393E-15	3.2850E-17	3.2850E-17
C2H8Si	1.6215E-15	2.7467E-17	2.7467E-17
C3ClH9Si	4.2519E-16	7.2022E-18	7.2022E-18
O2Si	2.5152E-16	4.2604E-18	4.2604E-18
H4O3Si	1.9471E-16	3.2981E-18	3.2981E-18
CClO	1.5450E-17	2.6170E-19	2.6170E-19
C2H6O	1.4059E-17	2.3815E-19	2.3815E-19
CCl2H	1.0166E-17	1.7219E-19	1.7219E-19
C3H6O	5.1114E-18	8.6582E-20	8.6582E-20
H2O3Si	4.7572E-18	8.0581E-20	8.0581E-20
H4O4Si	1.3125E-18	2.2233E-20	2.2233E-20
O2S	9.4224E-19	1.5961E-20	1.5961E-20
C2Cl2H4	5.7601E-19	9.7570E-21	9.7570E-21
Cl2S2	3.9315E-19	6.6596E-21	6.6596E-21
ClHO	6.0374E-20	1.0227E-21	1.0227E-21
CCl2O	4.0453E-20	6.8523E-22	6.8523E-22
CHO2	2.7578E-20	4.6714E-22	4.6714E-22
CCl3H	1.7280E-21	2.9270E-23	2.9270E-23
O	9.4386E-22	1.5988E-23	1.5988E-23
C2H6OSi	7.0494E-24	1.1941E-25	1.1941E-25
C2Cl3H	4.2980E-24	7.2803E-26	7.2803E-26
Cl2OS	4.1768E-25	7.0750E-27	7.0750E-27
C2Cl3H3	1.9545E-26	3.3107E-28	3.3107E-28
H2Na2O2	8.8877E-27	1.5055E-28	1.5055E-28
C2H6O2	7.3990E-28	1.2533E-29	1.2533E-29
Na2O	3.4142E-28	5.7832E-30	5.7832E-30
O2	3.0385E-28	5.1469E-30	5.1469E-30
CCl4	4.9486E-30	8.3824E-32	8.3824E-32
C2Cl4	2.6308E-32	4.4563E-34	4.4563E-34
C2Cl4H2	3.5045E-33	5.9363E-35	5.9363E-35
O3S	8.9698E-34	1.5194E-35	1.5194E-35
Cl2O2S	2.2278E-38	3.7736E-40	3.7736E-40
C2Cl5H	7.1475E-41	1.2107E-42	1.2107E-42
Na2O2	2.5330E-42	4.2906E-44	4.2906E-44
Na2O4S	1.0552E-43	1.7874E-45	1.7874E-45
C2Cl5	1.5737E-44	2.6657E-46	2.6657E-46
C2Cl6	5.8053E-49	9.8336E-51	9.8336E-51
TOTAL:	5.9036E+01	1.0000E+00	1.0000E+00

SOLID PHASES

Species	mol	ACTIVITY
CSi	5.1156E+01	1.0000E+00
O2Si	4.8830E+01	1.0000E+00
C	4.8753E+01	1.0000E+00
S2Si	0.0000E+00	1.4139E-01
ClNa	0.0000E+00	1.3113E-02
Si	0.0000E+00	1.1526E-03
S	0.0000E+00	1.1982E-04
NaS	0.0000E+00	8.4565E-07
Na2S	0.0000E+00	4.4608E-09
Na	0.0000E+00	1.2684E-09
Na2S2	0.0000E+00	6.2600E-10
Na2S2	0.0000E+00	6.2600E-10
Na2O5Si2	0.0000E+00	1.8579E-10
Cl4Si	0.0000E+00	1.8251E-10
HNaO	0.0000E+00	2.0836E-12
Na2S3	0.0000E+00	1.8078E-16
Na2O	0.0000E+00	3.3591E-21
Cl2S2	0.0000E+00	4.9773E-23
Na4O4Si	0.0000E+00	6.1903E-26
Na2O3S	0.0000E+00	8.5521E-33
Na2O4S	0.0000E+00	3.8421E-38
ClNaO4	0.0000E+00	<1.0000E-75

APPENDIX B

Condensed Results for Thermochemical Modeling of the Corrosion of SiC-Based Hot-Gas Filter Materials under the Conditions listed in Table 1. Summary Results are Given in Table 3

Table B1   Condensed equilibrium results for Argonne National Laboratory combustion gases present under: (a) oxidizing (1 atm, 850°C) and (b) reducing (1 atm, 650°C) conditions. No filter material is present. Details of conditions are given in Table 1.

Table B2   Condensed equilibrium results for Argonne National Laboratory combustion gases present under oxidizing (1 atm, 850°C) with (a) excess SiC filter material, and (b) excess SiO_2 after a protective oxide film separates the SiC from the gas. Details of conditions are given in Table 1.

Table B3   Condensed equilibrium results for Argonne National Laboratory combustion gases present under reducing (1 atm, 650°C) with (a) excess SiC filter material, and (b) excess SiO_2 after a protective oxide film separates the SiC from the gas. Details of conditions are given in Table 1.

Table B4   Condensed equilibrium results for Penn State gases present with (a) excess SiC filter material, and (b) excess SiO_2 after a protective oxide film separates the SiC from the gas. Details of conditions are given in Table 1.

Table B5   Condensed equilibrium results for Pinon Pines 1 atm combustion gases present with (a) excess SiC filter material, and (b) excess SiO_2 after a protective oxide film separates the SiC from the gas. Details of conditions are given in Table 1.

Table B6   Condensed equilibrium results for Pinon Pines 10 atm combustion gases present with (a) excess SiC filter material, and (b) excess SiO_2 after a protective oxide film separates the SiC from the gas. Details of conditions are given in Table 1.

Table B7   Condensed equilibrium results for Wilsonville 11.6 atm combustion gases present with (a) excess SiC filter material, and (b) excess SiO_2 after a protective oxide film separates the SiC from the gas. Details of conditions are given in Table 1.

Table B1a Argonne kes/psu 11/24/97
no filter (ox)

T = 850°C   P = 1.0 atm

INPUT SPECIES	AMOUNT/mol
N2/Gas/	7.24E+01
CO2/Gas/	1.35E+01
O2/Gas/	3.70E+00
H2O/Gas/	1.05E+01
O2S/Gas/	2.50E-02
ClNa/Gas/	5.00E-03

PHASE: Gas	PRESSURE atm
N2	7.23E-01
CO2	1.34E-01
H2O	1.04E-01
O2	3.69E-02
O2S	2.05E-04
ClH	4.84E-05
O3S	1.98E-05
ClNa	1.45E-06
CO	1.75E-09
H2	1.24E-09
TOTAL:	1.00E+00

SOLIDS	ACTIVITY
Na2O4S	1.00E+00
ClNa	1.60E-03

Table B1b B1a Argonne kes/psu 11/24/97
no filter (red)

T = 650°C   P = 1.0 atm

INPUT SPECIES	AMOUNT/mol
N2/Gas/	5.00E+01
CO2/Gas/	6.90E+00
CO/Gas/	8.80E+00
H2O/Gas/	2.40E+01
H2/Gas/	9.40E+00
ClNa/Gas/	5.00E-03

PHASE: Gas	PRESSURE atm
N2	5.04E-01
H2O	1.95E-01
H2	1.41E-01
CO2	1.16E-01
CO	4.14E-02
CH4	2.22E-04
ClNa	7.03E-06
ClH	1.15E-07
TOTAL:	1.00E+00

SOLIDS	ACTIVITY
ClNa	1.00E+00
HNaO	7.17E-02
C	4.68E-02

Table B2a Argonne (ox) kes/psu 11/24/97
T = 850°C   P = 1.0 atm

INPUT SPECIES	AMOUNT/mol
N2/Gas/	7.24E+01
CO2/Gas/	1.35E+01
O2/Gas/	3.70E+00
H2O/Gas/	1.05E+01
O2S/Gas/	2.50E-02
ClNa/Gas/	5.00E-03
*CSi	1.00E+02

PHASE: Gas	PRESSURE atm
N2	8.73E-01
H2	1.25E-01
CH4	4.72E-04
H2S	2.84E-04
ClNa	5.57E-05
SSi	1.73E-05
CO	6.82E-06
ClH	1.73E-06
H2O	5.72E-08
OSi	1.34E-09
TOTAL:	1.00E+00

SOLIDS	ACTIVITY
CSi	1.00E+00
C	1.00E+00
O2Si	1.00E+00
ClNa	6.15E-02
Na2S	3.97E-03
Na2O5Si2	1.23E-03

Table B2b Argonne (ox) kes/psu 11/24/97
T = 850°C   P = 1.0 atm

INPUT SPECIES	AMOUNT/mol
N2/Gas/	7.24E+01
CO2/Gas/	1.35E+01
O2/Gas/	3.70E+00
H2O/Gas/	1.05E+01
O2S/Gas/	2.50E-02
ClNa/Gas/	5.00E-03
*O2Si	1.00E+02

PHASE: Gas	PRESSURE atm
N2	7.23E-01
CO2	1.34E-01
H2O	1.04E-01
O2	3.69E-02
O2S	2.05E-04
ClH	4.84E-05
O3S	1.98E-05
ClNa	1.45E-06
Na2O4S	2.64E-08
H4O4Si	9.33E-09
CO	1.75E-09
H2	1.24E-09
TOTAL:	1.00E+00

SOLIDS	ACTIVITY
O2Si	1.00E+00
Na2O4S	1.00E+00
Na2O5Si2	1.99E-03
ClNa	1.60E-03

Table B3a Argonne (red) kes/psu 11/24/97
T = 650°C   P = 1.0 atm

INPUT SPECIES	AMOUNT/mol
N2/Gas/	5.00E+01
CO2/Gas/	6.90E+00
CO/Gas/	8.80E+00
H2O/Gas/	2.40E+01
H2/Gas/	9.40E+00
ClNa/Gas/	5.00E-03
*CSi	1.00E+02

PHASE: Gas	PRESSURE atm
N2	6.17E-01
H2	3.53E-01
CH4	2.96E-02
ClNa	7.03E-06
ClH	8.24E-08
CO	5.92E-09
H2O	3.26E-09
ClH3Si	1.10E-10
H4Si	7.74E-12
OSi	1.77E-13
CO2	1.11E-16
TOTAL:	1.00E+00

SOLIDS	ACTIVITY
CSi	1.00E+00
C	1.00E+00
O2Si	1.00E+00
ClNa	1.00E+00
Na2O5Si2	4.45E-02

Table B3b Argonne (red) kes/psu 11/24/97
T = 650°C   P = 1.0 atm

INPUT SPECIES	AMOUNT/mol
N2/Gas/	5.00E+01
CO2/Gas/	6.90E+00
CO/Gas/	8.80E+00
H2O/Gas/	2.40E+01
H2/Gas/	9.40E+00
ClNa/Gas/	5.00E-03
*O2Si	1.00E+02

PHASE: Gas	PRESSURE atm
N2	5.04E-01
H2O	1.95E-01
H2	1.41E-01
CO2	1.16E-01
CO	4.14E-02
CH4	2.22E-04
ClH	4.74E-05
ClNa	2.47E-06
H4O4Si	8.68E-09
TOTAL:	1.00E+00

SOLIDS	ACTIVITY
O2Si	1.00E+00
Na2O5Si2	1.00E+00
ClNa	3.52E-01
C	4.68E-02

Table B4a Penn State   kes/psu 11/24/97
T = 870°C   P = 1.0 atm

INPUT SPECIES	AMOUNT/mol
N2/Gas/	4.40E+01
O2/Gas/	4.10E+01
H2O/Gas/	1.50E+01
O2S/Gas/	3.30E-01
ClNa/Gas/	1.00E-03
ClH/Gas/	1.10E-01
*CSi	1.00E+02

PHASE: Gas	PRESSURE atm
N2	7.45E-01
H2	2.45E-01
H2S	5.34E-03
ClH	1.86E-03
CH4	1.53E-03
SSi	2.43E-04
ClNa	1.67E-05
CO	1.20E-05
ClH3Si	6.59E-07
HS	6.68E-07
H2O	1.53E-07
OSi	2.76E-09
TOTAL:	1.00E+00

SOLIDS	ACTIVITY
CSi	1.00E+00
O2Si	1.00E+00
C	1.00E+00
S2Si	1.41E-01
ClNa	1.31E-02

Table B4b Penn State   kes/psu 11/24/97
T = 870°C   P = 1.0 atm

INPUT SPECIES	AMOUNT/mol
N2/Gas/	4.40E+01
O2/Gas/	4.10E+01
H2O/Gas/	1.50E+01
O2S/Gas/	3.30E-01
ClNa/Gas/	1.00E-03
ClH/Gas/	1.10E-01
*O2Si	1.00E+02

PHASE: Gas	PRESSURE atm
N2	4.38E-01
O2	4.07E-01
H2O	1.49E-01
O2S	2.59E-03
ClH	1.09E-03
O3S	6.94E-04
ClNa	7.52E-06
Na2O4S	4.65E-08
H4O4Si	2.11E-08
H2	8.50E-10
TOTAL:	1.00E+00

SOLIDS	ACTIVITY
O2Si	1.00E+00
Na2O4S	1.00E+00
ClNa	5.89E-03
Na2O5Si2	1.06E-04

Table B5a Pinon Pine(1) kes/psu 11/24/97
T = 750°C   P = 1.0 atm

INPUT SPECIES	AMOUNT/mol
N2/Gas/	4.86E+01
CO2/Gas/	5.45E+00
CO/Gas/	2.38E+01
H2O/Gas/	5.51E+00
H2/Gas/	1.45E+01
H2S/Gas/	2.00E-03
CH4/Gas/	1.35E+00
*CSi	1.00E+02

PHASE: Gas	PRESSURE atm
N2	6.86E-01
H2	3.06E-01
CH4	7.21E-03
H2S	2.81E-05
CO	2.85E-07
SSi	8.49E-08
H2O	2.42E-08
OSi	2.41E-11
TOTAL:	**1.00E+00**

SOLIDS	ACTIVITY
CSi	1.00E+00
C	1.00E+00
O2Si	1.00E+00
Si	4.68E-04

Table B5b Pinon Pine(1) kes/psu 11/24/97
T = 750°C   P = 1.0 atm

INPUT SPECIES	AMOUNT/mol
N2/Gas/	4.86E+01
CO2/Gas/	5.45E+00
CO/Gas/	2.38E+01
H2O/Gas/	5.51E+00
H2/Gas/	1.45E+01
H2S/Gas/	2.00E-03
CH4/Gas/	1.35E+00
*O2Si	1.00E+02

PHASE: Gas	PRESSURE atm
N2	4.77E-01
CO	2.40E-01
H2	1.86E-01
CO2	5.97E-02
H2O	3.54E-02
CH4	9.28E-04
H2S	1.85E-05
COS	1.10E-06
H4O4Si	5.88E-10
TOTAL:	**1.00E+00**

SOLIDS	ACTIVITY
O2Si	1.00E+00
C	3.49E-01

Table B6a Pinon Pine(10) kes/psu 11/24/97
T = 750°C   P = 10.0 atm

INPUT SPECIES	AMOUNT/mol
N2/Gas/	4.86E+01
CO2/Gas/	5.45E+00
CO/Gas/	2.38E+01
H2O/Gas/	5.51E+00
H2/Gas/	1.45E+01
H2S/Gas/	2.00E-03
CH4/Gas/	1.35E+00
*CSi	1.00E+02

PHASE: Gas	PRESSURE atm
N2	7.11E+00
H2	2.42E+00
CH4	4.52E-01
H2S	2.92E-04
CO	2.85E-07
H2O	1.92E-07
SSi	1.11E-07
H4Si	1.24E-09
OSi	2.41E-11
TOTAL:	1.00E+00

SOLIDS	ACTIVITY
CSi	1.00E+00
C	1.00E+00
O2Si	1.00E+00
Si	4.68E-04
S2Si	1.71E-05

Table B6b Pinon Pine(10) kes/psu 11/24/97
T = 750°C   P = 10.0 atm

INPUT SPECIES	AMOUNT/mol
N2/Gas/	4.86E+01
CO2/Gas/	5.45E+00
CO/Gas/	2.38E+01
H2O/Gas/	5.51E+00
H2/Gas/	1.45E+01
H2S/Gas/	2.00E-03
CH4/Gas/	1.35E+00
*O2Si	1.00E+02

PHASE: Gas	PRESSURE atm
N2	5.13E+00
CO	1.64E+00
H2	1.43E+00
CO2	9.76E-01
H2O	6.53E-01
CH4	1.57E-01
H2S	2.00E-04
COS	1.05E-05
H4O4Si	1.99E-07
TOTAL:	1.00E+01

SOLIDS	ACTIVITY
O2Si	1.00E+00
C	1.00E+00

Table B7a Wilsonville
T = 816°C   kes/psu 11/24/97   P = 11.6 atm

INPUT SPECIES	AMOUNT/mol
N2/Gas/	5.2600E+01
CO2/Gas/	2.3700E+01
CO/Gas/	6.8000E+00
H2O/Gas/	1.2500E+01
H2/Gas/	5.0000E-01
H2S/Gas/	8.0000E-02
ClNa/Gas/	3.0000E-03
CH4/Gas/	1.6000E+00
COS/Gas/	1.5000E-02
*CSi	1.0000E+02

PHASE: Gas	PRESSURE atm
N2	9.02E+00
H2	2.33E+00
CH4	2.21E-01
H2S	1.62E-02
ClNa	3.22E-04
SSi	2.72E-05
ClH	6.25E-06
CO	2.47E-06
H2O	6.09E-07
OSi	3.73E-10
TOTAL:	1.00E+00

SOLIDS	ACTIVITY
CSi	1.00E+00
C	1.00E+00
O2Si	1.00E+00
Na2S	9.71E-01
ClNa	6.60E-01
Na2O5Si2	6.33E-02

Table B7b Wilsonville
T = 816°C   kes/psu 11/24/97   P = 11.6 atm

INPUT SPECIES	AMOUNT/mol
N2/Gas/	5.26E+01
CO2/Gas/	2.37E+01
CO/Gas/	6.80E+00
H2O/Gas/	1.25E+01
H2/Gas/	5.00E-01
H2S/Gas/	8.00E-02
ClNa/Gas/	3.00E-03
CH4/Gas/	1.60E+00
COS/Gas/	1.50E-02
*O2Si	1.00E+02

PHASE: Gas	PRESSURE atm
N2	6.04E+00
CO2	2.64E+00
H2O	1.32E+00
CO	1.03E+00
H2	5.32E-01
H2S	1.00E-02
COS	8.77E-04
CH4	5.03E-04
ClH	2.99E-04
ClNa	4.16E-05
H4O4Si	1.23E-06
TOTAL:	1.00E+00

SOLIDS	ACTIVITY
O2Si	1.00E+00
Na2O5Si2	1.00E+00
ClNa	8.53E-02
C	4.39E-02

APPENDIX C

Condensed Results for Thermochemical Modeling of the Corrosion of Alumina/Mullite Hot-Gas Filter Materials under the Conditions listed in Table 1. Summary Results are Given in Table 4.

Table C1   Condensed equilibrium results for Argonne National Laboratory combustion gases present under oxidizing (1 atm, 850°C) conditions with excess Alumina/Mullite filter material. Details of conditions are given in Table 1.

Table C2   Condensed equilibrium results for Argonne National Laboratory combustion gases present under reducing (1 atm, 650°C) conditions with excess Alumina/Mullite filter material. Details of conditions are given in Table 1.

Table C3   Condensed equilibrium results for Penn State gases present with excess Alumina/Mullite filter material. Details of conditions are given in Table 1.

Table C4   Condensed equilibrium results for Pinon Pine 1 atm combustion gases present with excess Alumina/Mullite filter material. Details of conditions are given in Table 1.

Table C5   Condensed equilibrium results for Pinon Pine 10 atm combustion gases present with excess Alumina/Mullite filter material. Details of conditions are given in Table 1.

Table C6   Condensed equilibrium results for Wilsonville 11.6 atm combustion gases present with excess Alumina/Mullite filter material. Details of conditions are given in Table 1.

Table C1 Argonne(ox) kes/psu 11/24/97
T = 850°C P = 1.0 atm

INPUT SPECIES	AMOUNT/mol
N2/Gas/	7.24E+01
CO2/Gas/	1.35E+01
O2/Gas/	3.70E+00
H2O/Gas/	1.05E+01
O2S/Gas/	2.50E-02
ClNa/Gas/	5.00E-03
*Al2O3	1.00E+02
*Al6O13Si2(MUL)	1.00E+02

PHASE: Gas	PRESSURE atm
N2	7.23E-01
CO2	1.34E-01
H2O	1.04E-01
O2	3.69E-02
O2S	2.27E-04
ClH	4.90E-05
O3S	2.20E-05
ClNa	8.19E-07
H4O4Si	5.25E-09
CO	1.75E-09
H2	1.24E-09
AlH3O3	2.87E-11
TOTAL:	1.00E+00

SOLIDS	ACTIVITY
Al2O3	1.00E+00
Al6O13Si2	1.00E+00
AlNaO4Si	1.00E+00
O2Si	5.62E-01
Na2O4S	3.40E-01

Table C2 Argonne(red) kes/psu 11/24/97
T = 650°C P = 1.0 atm

INPUT SPECIES	AMOUNT/mol
N2/Gas/	5.00E+01
CO2/Gas/	6.90E+00
CO/Gas/	8.80E+00
H2O/Gas/	2.40E+01
H2/Gas/	9.40E+00
ClNa/Gas/	5.00E-03
*Al2O3	1.00E+02
*Al6O13Si2(MUL)	1.00E+02

PHASE: Gas	PRESSURE atm
N2	5.04E-01
H2O	1.95E-01
H2	1.41E-01
CO2	1.16E-01
CO	4.14E-02
CH4	2.22E-04
ClH	5.04E-05
ClNa	3.77E-08
H4O4Si	4.06E-09
AlH3O3	8.90E-13
TOTAL:	1.00E+00

SOLIDS	ACTIVITY
Al2O3	1.00E+00
Al6O13Si2	1.00E+00
AlNaO4Si	1.00E+00
O2Si	4.67E-01
C	4.68E-02

Table C3   Penn State
T = 870°C   kes/psu 11/24/97
                 P = 1.0 atm

INPUT SPECIES	AMOUNT/mol
N2/Gas/	4.40E+01
O2/Gas/	4.10E+01
H2O/Gas/	1.50E+01
O2S/Gas/	3.30E-01
ClNa/Gas/	1.00E-03
ClH/Gas/	1.10E-01
*Al2O3	1.00E+02
*Al6O13Si2(MUL)	1.00E+02

PHASE: Gas	PRESSURE atm
N2	4.38E-01
O2	4.07E-01
H2O	1.49E-01
O2S	2.59E-03
ClH	1.09E-03
O3S	6.94E-04
ClNa	7.52E-06
Na2O4S	4.65E-08
H4O4Si	1.16E-08
AlH3O3	6.99E-11
TOTAL:	**1.00E+00**

SOLIDS	ACTIVITY
Al2O3	1.00E+00
Al6O13Si2	1.00E+00
Na2O4S	1.00E+00
O2Si	5.49E-01
AlNaO4Si	3.80E-01

Table C4   Pinon Pine(1)   kes/psu 11/24/97
T = 750°C   P = 1.0 atm

INPUT SPECIES	AMOUNT/mol
N2/Gas/	4.86E+01
CO2/Gas/	5.45E+00
CO/Gas/	2.38E+01
H2O/Gas/	5.51E+00
H2/Gas/	1.45E+01
H2S/Gas/	2.00E-03
CH4/Gas/	1.35E+00
*Al2O3	1.00E+02
*Al6O13Si2(MUL)	1.00E+02

PHASE: Gas	PRESSURE atm
N2	4.77E-01
CO	2.40E-01
H2	1.86E-01
CO2	5.97E-02
H2O	3.54E-02
CH4	9.28E-04
H2S	1.85E-05
COS	1.09E-06
H4O4Si	3.04E-10
AlH3O3	7.72E-13
TOTAL:	**1.00E+00**

SOLIDS	ACTIVITY
Al2O3	1.00E+00
Al6O13Si2	1.00E+00
O2Si	5.18E-01
C	3.49E-01

Table C5 Pinon Pine(10) kes/psu 11/24/97
T = 750°C P = 10.0 atm

INPUT SPECIES	AMOUNT/mol
N2/Gas/	4.86E+01
CO2/Gas/	5.45E+00
CO/Gas/	2.38E+01
H2O/Gas/	5.51E+00
H2/Gas/	1.45E+01
H2S/Gas/	2.00E-03
CH4/Gas/	1.35E+00
*Al2O3	1.00E+02
*Al6O13Si2(MUL)	1.00E+02

PHASE: Gas	PRESSURE atm
N2	5.13E+00
CO	1.64E+00
H2	1.43E+00
CO2	9.76E-01
H2O	6.53E-01
CH4	1.57E-01
H2S	2.00E-04
COS	1.05E-05
H4O4Si	1.03E-07
AlH3O3	6.10E-11
TOTAL:	1.00E+00

SOLIDS	ACTIVITY
Al2O3	1.00E+00
Al6O13Si2	1.00E+00
C	1.00E+00
O2Si	5.18E-01

Table C6 Wilsonvilole kes/psu 11/24/97
T = 816°C P = 11.6 atm

INPUT SPECIES	AMOUNT/mol
N2/Gas/	5.26E+01
CO2/Gas/	2.37E+01
CO/Gas/	6.80E+00
H2O/Gas/	1.25E+01
H2/Gas/	5.00E-01
H2S/Gas/	8.00E-02
ClNa/Gas/	3.00E-03
CH4/Gas/	1.60E+00
COS/Gas/	1.50E-02
*Al2O3	1.00E+02
*Al6O13Si2(MUL)	1.00E+02

PHASE: Gas	PRESSURE atm
N2	6.04E+00
CO2	2.64E+00
H2O	1.32E+00
CO	1.03E+00
H2	5.32E-01
H2S	1.00E-02
COS	8.77E-04
CH4	5.03E-04
ClH	3.43E-04
ClNa	1.08E-06
H4O4Si	6.77E-07
AlH3O3	6.85E-10
TOTAL:	1.00E+0

SOLIDS	ACTIVITY
Al2O3	1.00E+00
Al6O13Si2	1.00E+00
AlNaO4Si	1.00E+00
O2Si	5.48E-01
C	4.39E-02

3M COMPANY
Ceramic Materials Department
201-4N-01 3M Center,
St. Paul, MN 55144
M. A. Leitheiser

AIR PRODUCTS AND CHEMICALS
P.O. Box 538
Allentown, PA 18105
S. W. Dean

ALLISON GAS TURBINE DIVISION
P.O. Box 420
Indianapolis, IN 46206-0420
P. Khandelwal (Speed Code W-5)
R. A. Wenglarz (Speed Code W-16)

AMA RESEARCH & DEVELOPMENT CENTER
5950 McIntyre Street
Golden, CO 80403
T. B. Cox

ARGONNE NATIONAL LABORATORY
9700 S. Cass Avenue
Argonne, IL 60439
W. A. Ellingson
J. P. Singh

BABCOCK & WILCOX
Domestic Fossil Operations
20 South Van Buren Avenue
Barberton, OH 44023
M. Gold

BRITISH COAL CORPORATION
Coal Technology Development Division
Stoke Orchard, Cheltenham
Glocestershire, England GL52 4ZG
J. Oakey

CANADA CENTER FOR MINERAL & ENERGY
TECHNOLOGY
568 Booth Street
Ottawa, Ontario
Canada K1A OG1
R. Winston Revic
Mahi Sahoo

DOE
DOE OAK RIDGE OPERATIONS
P.O.Box 2001
Oak Ridge, TN 37831
Assistant Manager for
Energy Research and Development

DOE
DOE OAK RIDGE OPERATIONS
P. O. Box 2008
Building 4500N, MS 6269
Oak Ridge, TN 37831
M. H. Rawlins

DOE
OFFICE OF BASIC ENERGY SCIENCES
Materials Sciences Division
ER-131
19901 Germantown Road
Germantown, MD 20874-1290
H. M. Kerch

DOE
IDAHO OPERATIONS OFFICE
P. O. Box 1625
Idaho Falls, ID 83415
J. B. Malmo

DOE
MORGANTOWN ENERGY TECHNOLOGY CENTER
P.O. Box 880
Morgantown, WV 26505
R. C. Bedick
D. C. Cicero
F. W. Crouse, Jr.
R. A. Dennis
N. T. Holcombe
W. J. Huber
T. J. McMahon
J. E. Notestein

DOE
OFFICE OF FOSSIL ENERGY
FE-72
19901 Germantown Road
Germantown, MD 20874-1290
F. M. Glaser

DOE
OFFICE OF VEHICLE AND ENERGY R&D
CE-151 Forrestal Building
Washington, DC 20585
R. B. Schulz

DOE
PITTSBURGH ENERGY TECHNOLOGY CENTER
P.O. Box 10940
Pittsburgh, PA 15236
A. L. Baldwin
G. V. McGurl
L. A. Ruth
T. M. Torkos

DOW CORNING CORPORATION
3901 S. Saginaw Road
Midland, MI 48686-0995
H. Atwell

EC TECHNOLOGIES
3614 Highpoint Drive
San Antonio, TX 78217
D. J. Kenton

ELECTRIC POWER RESEARCH INSTITUTE
P.O. Box 10412
3412 Hillview Avenue
Palo Alto, CA 94303
W. T. Bakker
J. Stringer

EUROPEAN COMMUNITIES JOINT RESEARCH
CENTRE
Petten Establishment
P.O. Box 2
1755 ZG Petten
The Netherlands
M. Van de Voorde

GEORGIA INSTITUTE OF TECHNOLOGY
Materials Science & Engineering (0245)
Bunger-Henry Building, Room 276
Atlanta, GA 30332-0245
T. L. Starr

IDAHO NATIONAL ENGINEERING LABORATORY
P. O. Box 1625
Idaho Falls, ID 83415
B. H. Rabin

LAWRENCE LIVERMORE NATIONAL LABORATORY
P.O. Box 808, L-325
Livermore, CA 94550
W. A. Steele

NATIONAL MATERIALS ADVISORY BOARD
National Research Council
2101 Constitution Avenue
Washington, DC 20418
K. M. Zwilsky

OAK RIDGE NATIONAL LABORATORY
P.O. Box 2008
Oak Ridge, TN 37831
P. T. Carlson
F. D. Johnson **(4 copies)**
R. R. Judkins
D. P. Stinton
M. R. Upton

OFFICE OF NAVAL RESEARCH
Code 431, 800 N. Quincy Street
Arlington, VA 22217
S. G. Fishman

SHELL DEVELOPMENT COMPANY
WTC R-1371
P.O. Box 1380
Houston, TX 77251-1380
W. C. Fort

TENNESSEE VALLEY AUTHORITY
Energy Demonstration & Technology
MR2N58A
Chattanooga, TN 37402-2801
C. M. Huang

THE JOHNS HOPKINS UNIVERSITY
Materials Science & Engineering
Maryland Hall
Baltimore, MD 21218
R. E. Green, Jr.

THE MATERIALS PROPERTIES COUNCIL, INC.
United Engineering Center
345 E. Forty-Seventh Street
New York, NY 10017
M. Prager

THE NORTON COMPANY
High Performance Ceramics Division
Goddard Road
Northborough, MA 01532-1545
N. Corbin

THE TORRINGTON COMPANY
Advanced Technology Center
59 Field St.
Torrington, CT 06790
W. J. Chmura

UNION CARBIDE CORPORATION
Linde Division
P.O. Box 44
175 East Park Drive
Tonawanda, NY 14151-0044
Harry Cheung

UNITED TECHNOLOGIES RESEARCH CENTER
MS 24, Silver Lane
East Hartford, CT 06108
K. M. Prewo

UNIVERSITY OF TENNESSEE
Dept of Materials Science and Engineering
Knoxville, TN 37996-2200
Peter Liaw

UNIVERSITY OF WASHINGTON
Department of Materials Science and
Engineering
101 Wilson, FB-10
Seattle, WA 98195
T. G. Stoebe

VIRGINIA POLYTECHNIC INSTITUTE & STATE
UNIVERSITY
Department of Materials Engineering
Blacksburg, VA 24601
K. L. Reifsnider

WESTERN RESEARCH INSTITUTE
365 N. 9th Street
P.O. Box 3395
University Station
Laramie, WY 82071
V. K. Sethi

WESTINGHOUSE ELECTRIC CORPORATION
Research and Development Center
1310 Beulah Road
Pittsburgh, PA 15235
S. C. Singhal